



**HAL**  
open science

## Combined effects of okadaic acid and pectenotoxin-2, 13-desmethylspirolide C or yessotoxin in human intestinal Caco-2 cells

Jimmy H Alarcán, Sabrina Barbé, Benjamin Kopp, Stefanie Hessel-Pras, Albert Braeuning, Alfonso Lampen, Ludovic Le Hegarat, Valérie Fessard

► **To cite this version:**

Jimmy H Alarcán, Sabrina Barbé, Benjamin Kopp, Stefanie Hessel-Pras, Albert Braeuning, et al.. Combined effects of okadaic acid and pectenotoxin-2, 13-desmethylspirolide C or yessotoxin in human intestinal Caco-2 cells. *Chemosphere*, 2019, 228, pp.139-148. 10.1016/j.chemosphere.2019.04.018 . anses-02114281

**HAL Id: anses-02114281**

**<https://anses.hal.science/anses-02114281>**

Submitted on 22 Oct 2021

**HAL** is a multi-disciplinary open access archive for the deposit and dissemination of scientific research documents, whether they are published or not. The documents may come from teaching and research institutions in France or abroad, or from public or private research centers.

L'archive ouverte pluridisciplinaire **HAL**, est destinée au dépôt et à la diffusion de documents scientifiques de niveau recherche, publiés ou non, émanant des établissements d'enseignement et de recherche français ou étrangers, des laboratoires publics ou privés.



Distributed under a Creative Commons Attribution - NonCommercial 4.0 International License

# 1 **Combined effects of okadaic acid and pectenotoxin-2, 13-desmethylspirolide** 2 **C or yessotoxin in human intestinal Caco-2 cells**

3  
4 Jimmy Alarcan<sup>1,2</sup>, Sabrina Barbé<sup>1</sup>, Benjamin Kopp<sup>1</sup>, Stefanie Hessel-Pras<sup>2</sup>, Albert Braeuning<sup>2</sup>, Alfonso  
5 Lampen<sup>2</sup>, Ludovic Le Hégarat<sup>1\*</sup> and Valérie Fessard<sup>1</sup>

6 <sup>1</sup> ANSES, French Agency for Food, Environmental and Occupational Health & Safety,  
7 Fougères-Laboratory, Toxicology of Contaminants Unit, 10B rue Claude Bourgelat, 35306 Fougères,  
8 France; jimmy.alarcan@anses.fr; sabrina.barbe.53@gmail.com; benjamin.kopp@anses.fr;  
9 valerie.fessard@anses.fr; ludovic.lehegarat@anses.fr

10 <sup>2</sup> German Federal Institute for Risk Assessment, Department of Food Safety, Max-Dohrn-Straße  
11 8-10, 10589 Berlin, Germany; Jimmy.Alarcan@bfr.bund.de (J.A); Stefanie.Hessel-Pras@bfr.bund.de  
12 (S.H-P.); Albert.Braeuning@bfr.bund.de (A.B.); Alfonso.Lampen@bfr.bund.de (A.L.)

13 \* Correspondence: ludovic.lehegarat@anses.fr; Tel.: +33-2-99-17-27-47; Adress: ANSES,  
14 French Agency for Food, Environmental and Occupational Health & Safety, Fougères Laboratory,  
15 Toxicology of contaminants Unit, 10B rue Claude Bourgelat, 35306 Fougères, France.

16

## 17 **Abstract (150-250 words)**

18 Lipophilic phycotoxins are secondary metabolites produced by phytoplanktonic species. They  
19 accumulate in filtering shellfish and can cause human intoxications. Humans can be exposed to  
20 combinations of several phycotoxins. The toxicological effects of phycotoxin mixtures on human  
21 health are largely unknown. Published data on phycotoxin co-exposure show that okadaic acid (OA) is  
22 simultaneously found with pectenotoxin-2 (PTX-2), 13-desmethylspirolide C (also known as SPX-1),  
23 or yessotoxin (YTX). Therefore, the aim of this study was to examine the effects of three binary  
24 mixtures, OA/PTX-2, OA/SPX-1 and OA/YTX on human intestinal Caco-2 cells. A multi-parametric  
25 approach for cytotoxicity determination was applied using a high-content analysis platform, including  
26 markers for cell viability, oxidative stress, inflammation, and DNA damage. Mixtures effects were  
27 analyzed using two additivity mathematical models. Our assays revealed that OA induced cytotoxicity,  
28 DNA strand breaks and interleukin 8 release. PTX-2 slightly induced DNA strand breaks, whereas  
29 SPX-1 and YTX did not affect the investigated endpoints. The combination of OA with another toxin  
30 resulted in reduced toxicity at low concentrations, suggesting antagonistic effects, but in increased  
31 effects at higher concentrations, suggesting additive or synergistic effects. Taken together, our results  
32 demonstrated that the cytotoxic effects of binary mixtures of lipophilic phycotoxins could not be  
33 predicted by additivity mathematical models. In conclusion, the present data suggest that combined  
34 effects of phycotoxins may occur which might have the potential to impact on risk assessment of these  
35 compounds.

36

37 **Keywords:** phycotoxins, mixtures, antagonism, synergism, genotoxicity, inflammation

38 **Abbreviations<sup>1</sup>:** ABC: ATP-binding cassette transporter; ADME: absorption, distribution,  
39 metabolism, excretion; CI: combination index; CYP: cytochrome P450; DSP: diarrhetic shellfish  
40 poisoning; EFSA: European Food Safety Authority; IL-8: interleukin 8; OA: okadaic acid; P-gp: P-  
41 glycoprotein; PP2A: protein phosphatase 2A; PTX-2: pectenotoxin-2; PXR: pregnane-X-receptor;  
42 ROS: reactive oxygen species; SM: shellfish meat; SPX-1: 13-desmethylspirolide C; TEF: toxicity  
43 equivalent factor; YTX: yessotoxin.

44

## 45 **1. Introduction (750 words)**

46 Marine biotoxins are secondary metabolites produced by specific phytoplanktonic species (Visciano et  
47 al., 2016). Among the lipophilic marine biotoxins, four main families have been described: okadaic  
48 acid (OA) and dinophysistoxins (DTXs), pectenotoxins (PTXs), yessotoxins (YTXs) and finally cyclic  
49 imines (including spirolides, pinnatoxins, pteriatoxins and gymnodimines). OA and DTXs are  
50 responsible for diarrhetic shellfish poisoning (DSP), characterized by diarrhea, nausea, abdominal pain  
51 and vomiting (Valdiglesias et al., 2013). The OA group of toxins inhibits serine/threonine protein  
52 phosphatase 2A (PP2A) and, to a lesser extent, also PP1 (Takai et al., 1992). The group of PTXs,  
53 principally PTX-2, is not anymore considered a DSP toxin since its implication in gastro-intestinal  
54 symptoms is not clear (Ito et al., 2008). At the cellular level, PTX-2 provokes actin depolarization  
55 leading to a disruption of the cytoskeleton (Alligham et al., 2007). The group of YTXs has no recorded  
56 effects in humans but has been frequently found together with OA in shellfish (Alarcan et al., 2018).  
57 YTX displays *in vitro* toxicity, for instance apoptosis induction and disturbance of the calcium flux  
58 (Tubaro et al., 2008). Its mechanism of action is still unknown but some studies suggest a possible  
59 connection with autophagy (Fernández-Araujo et al., 2015). Finally, potent neurological effects in  
60 mice have been reported for the group of cyclic imines (Munday et al., 2012). SPX-1 is a selective  
61 inhibitor of nicotinic acetylcholine receptors (Araoz et al., 2015).

62 For some of them, regulatory limits were set to protect consumers from their potential harm as they  
63 can contaminate shellfish and be responsible for foodborne outbreaks (EFSA report 2009). OA and  
64 PTX-2 together share a limit of 160 µg /kg shellfish meat (SM), and for YTX and its analogues the  
65 limit is set to 3.75 mg YTX eq/kg SM. However, in the absence of reports on human intoxications, no  
66 regulatory limits have been established for the group of cyclic imines, even though they are frequently  
67 detected in shellfish and can be very toxic to mice following intra-peritoneal or oral administration  
68 (Munday et al., 2012). Mixtures of marine biotoxins are only regarded by the abovementioned EFSA  
69 opinion in case of toxin analogs with established toxicity equivalent factors (TEFs). However, studies  
70 regarding deleterious effects generated by the mixtures of toxins from different chemical groups are  
71 lacking. Therefore the impact of toxin co-occurrence on toxicity needs to be more deeply investigated.

72

73 A high number of different approaches have been described to analyze the combined effects of  
74 mixtures (Fouquier and Guedj 2015). Even though antagonism and synergism are well-established

---

<sup>1</sup>**Abbreviations:** ABC: ATP-binding cassette transporter; ADME: absorption, distribution, metabolism,  
excretion; CI: combination index; CYP: cytochrome P450; DSP: diarrhetic shellfish poisoning; EFSA: European  
Food Safety Authority; IL-8: interleukin 8; OA: okadaic acid; P-gp: P-glycoprotein; PP2A: protein phosphatase  
2A; PTX-2: pectenotoxin-2; PXR: pregnane-X-receptor; ROS: reactive oxygen species; SPX-1: 13-  
desmethylspirolide C; TEF: toxicity equivalent factor; YTX: yessotoxin.

75 concepts, the definition of additivity is broad (Foucquier and Guedj, 2015) resulting in several  
76 proposed models. Generally speaking, additivity models allow predicting the additive effects of a  
77 mixture from the toxicity of each component. They assume that each component exerts an effect  
78 without influencing the action of the other ones. Deviation from predicted additivity is considered as  
79 synergism or antagonism. The two main concepts used are concentration addition (CA) and  
80 independent action (IA). The CA concept relies on the assumption that the components in the mixture  
81 act on the same biological sites, by the same mechanisms of action and differ only in their potency  
82 (Loewe and Muischnek, 1926). The IA concept established by Bliss (1939) relies on the hypothesis  
83 that a combined effect can be calculated from the responses of the individual mixture components,  
84 assuming that each one acts independently without interfering with the others (different sites of  
85 action).

86 So far, only few studies have been undertaken with mixtures of phycotoxins. No combined effects  
87 were reported in rodents except in the distribution into internal organs where a reduced level was  
88 observed in case of mixtures (Aasen et al., 2011; Sosa et al., 2013). In human neuroblastoma cells, OA  
89 co-incubated with YTX or SPX-1 showed additive effect towards cell viability (Rodriguez et al.,  
90 2015). However, on proliferative human intestinal epithelial cells, binary combinations of azaspiracid-  
91 1 (AZA-1)/OA and YTX/OA resulted in an increasing antagonistic effect on viability when toxin  
92 concentrations raised, whereas AZA-1/YTX mixtures showed dose-dependent synergism (Ferron et  
93 al., 2016).

94 In this study we chose relevant mixtures based on our recently published review (Alarcan et al., 2018),  
95 highlighting that OA was predominantly found as the main toxin combined with PTX-2, YTX or SPX-  
96 1. Our objective was to complete the previous data by assessing a panel of different toxicity endpoints  
97 (cell viability, oxidative stress, inflammation, and DNA strand breaks) in the human Caco-2 cell line  
98 with binary mixtures of lipophilic toxins.

99

## 100 **2. Materials and methods**

### 101 **2.1 Establishment of mixtures**

102 Three binary mixtures were selected in the following molar ratios according to published literature on  
103 lipophilic phycotoxins co-exposure (Alarcan et al., 2018): 3:1 for OA/PTX-2 and OA/YTX and 9:1 for  
104 OA/SPX-1. Concentrations ranges were established based on preliminary cell viability experiments  
105 and published data. PTX-2, YTX and SPX-1 did not show any cytotoxicity (NRU, DAPI cell count)  
106 after 24h on differentiated Caco-2 cells up to 500, 200 and 510 nM, respectively (unpublished data).  
107 Based on the cytotoxicity results (MTT assay) for OA reported by Ehlers et al. (2011), a maximum  
108 concentration of 600 nM was chosen in order to study biological responses in both cytotoxic and non-  
109 cytotoxic conditions. Then, based on the ratios of toxins previously indicated, we deduced the  
110 concentrations for PTX-2, YTX and SPX-1 from those chosen for OA.

### 111 **2.2 Chemicals**

112 Toxin standards were purchased from the National Research Council Institute for Marine Biosciences  
113 (Halifax, NS Canada). DCFH-DA, potassium bromate (KBrO<sub>3</sub>), sulfuric acid (H<sub>2</sub>SO<sub>4</sub>) and TNF $\alpha$  were  
114 purchased from Sigma-Aldrich (St. Louis, MO, USA). Primary anti-interleukin 8 (IL-8) antibody  
115 (M801), biotin-conjugated human IL-8 (M802B), HRP-conjugated streptavidin (N100), and 3,3',5,5'-  
116 tetramethylbenzidine (TMB) were obtained from Thermo Fisher Scientific (Waltham, MA, USA).  
117 Mouse monoclonal anti  $\gamma$ H2AX S19 (ab26350) and goat pAb to Ms IgG Alexa Fluor 647 (ab150115)

118 were purchased from Abcam (Cambridge, UK). All other chemicals including ethanol (EtOH),  
119 methanol (MeOH) and dimethyl sulfoxide (DMSO) were of analytical grade and purchased from  
120 Fisher Scientific (Leicestershire, England). Deionised water was prepared using a Milli-Q system  
121 (Millipore, Bedford, MA, USA).

## 122 **2.3 Cell culture**

123 Caco-2 cells were obtained from the American Type Culture Collection HTB-37 (LGC Standards,  
124 Molsheim, France). Cells (passages 30–38) were seeded at 10,000 cells/cm<sup>2</sup> in 96-well plates in  
125 culture medium (minimum essential medium, supplemented with 10% fetal calf serum, 1% non-  
126 essential amino acids, 50 IU/ml penicillin and 50 µg/ml streptomycin) and maintained at 37 °C under  
127 5% CO<sub>2</sub>. Media, serum, amino acids solution and antibiotics were all from Invitrogen (Saint Aubin,  
128 France). For differentiation into an intestinal epithelial-like monolayer, cells were cultured for 3 weeks  
129 with renewal of medium every 2 to 3 days (Sambuy et al., 2005). All the assays were performed on  
130 differentiated Caco-2 cells.

## 131 **2.4 Measurement of ROS production**

132 ROS were measured using the probe DCFH-DA. Caco-2 cells were pre-treated with 25 µM DCFH-  
133 DA for 30 min. The culture medium was then removed and medium containing the toxins was added  
134 for 24 h of incubation at 37°C. Fluorescence was measured at  $\lambda_{ext} = 485 \text{ nm}$  and  $\lambda_{em} = 520 \text{ nm}$   
135 using a Fluostar Omega microplate reader (BMG Labtek).

## 136 **2.5 Cell viability and DNA strand breaks**

137 After 24 h of treatment with the toxins, Caco-2 cells were fixed with 4% paraformaldehyde in  
138 phosphate-buffered saline (PBS) for 10 min and permeabilized with 0.2% Triton X-100 for 15 min.  
139 Plates were then incubated in blocking solution (PBS with 1% BSA and 0.05% Tween-20) for 30 min  
140 before the addition of primary antibody prepared in blocking solution and filtered with a 0.2 µm  
141 syringe filter. Mouse monoclonal anti  $\gamma$ H2AX S19 (1:1000 dilution) was incubated with the cells for  
142 1.5 h at room temperature. After washing with PBS + 0.05% Tween-20, goat pAb to Ms IgG Alexa  
143 Fluor 647 (1:1000) was added for 45 min incubation at room temperature. Nuclear DAPI (1 µg/mL)  
144 staining was used for automated cell identification by high content analysis. Plates were scanned with  
145 the Thermo Scientific ArrayScan VTI HCS Reader (Thermo Scientific, Waltham, USA) and analyzed  
146 using the Target Activation module of the BioApplication software. For each well, 10 fields (10X  
147 magnification) were scanned and analyzed for immunofluorescence quantification. Cell counts were  
148 determined by DAPI staining.  $\gamma$ -H2AX was quantified in the nuclei and expressed as fold increase  
149 compared to solvent controls. No  $\gamma$ -H2AX data are provided for toxin concentrations resulting in a cell  
150 viability < 40%, to ensure a reliable measurement of DNA damage.

## 151 **2.6 IL-8 release by ELISA**

152 After treatment with toxins, cell culture supernatants were collected and analyzed for IL-8 release.  
153 Samples were transferred to 96-well microplates coated overnight at 4°C with 1 µg/mL human  
154 recombinant anti-IL-8 primary antibody. Following addition of 0.1 µg/mL of the biotin-conjugated  
155 human IL-8 antibody for 1 h, streptavidin peroxidase (1:10000) was added for 45 min. After washing  
156 with PBS + 0.05% Tween-20, 3,3',5,5'-tetramethylbenzidine (TMB) solution was added to initiate the  
157 colorimetric reaction. The reaction was stopped by 1 M H<sub>2</sub>SO<sub>4</sub> and absorbance was measured at 405  
158 nm using a Fluostar Omega microplate reader (BMG Labtek).

## 159 **2.7 Statistics/Data analysis**

160 GraphPad Prism 5 (GraphPad Software, Inc) was used for statistical analyses. Two-way ANOVA  
161 followed by Bonferroni's post-hoc tests were used to compare the effects of toxins and solvent control  
162 All error bars denote standard error of the mean (SEM). Symbols \*, \*\*, \*\*\*, \*\*\*\* and #, ##, ###,  
163 ##### indicate statistical significance between toxin and solvent control or OA and mixture  
164 respectively (p < 0.05, p < 0.01, p < 0.001, p < 0.0001 respectively).

## 165 **2.8 Mixture effects predictions using additivity models**

166 Since the tested phycotoxins do not share any known common mechanism of action, using the CA  
167 concept is therefore not relevant. Instead, the mathematical definition of additivity, also known as  
168 theoretical additivity, response additivity or linear interaction effect, was employed (Fouquier and  
169 Guedj, 2015). The independent action concept was also employed.

### 170 **2.8.1 Theoretical additivity method**

171 The theoretical additivity (TA) method was used as described by Weber et al., (2005). This method  
172 compares theoretical predicted values calculated from the results of each individual compound to the  
173 measured values obtained with mixtures. In our study of binary phycotoxin combinations, the  
174 predicted mixture effect values were calculated as follows:

175 *Mix(A + B)predicted value = (mean value A + mean value B) – mean value solvent control*

176  
177 For data expressed as fold change compared to solvent control, mean value solvent control = 1 while  
178 for cell viability analysis, the mean value for the solvent control was set to 100.

179 Combination index (CI), a standard measure of combination effect, was calculated as indicated by  
180 Fouquier and Guedj (2015):

$$181 \quad CI = \frac{Mix(A + B)predicted\ value}{Mix(A + B)measured\ value}$$

182 Threshold of the computed CI of  $CI < 0.9$ ,  $0.9 \leq CI \leq 1.1$ , and  $CI > 1.1$  were set to indicate synergism,  
183 additive effects and antagonism, respectively. In order to get cell viability CI values that respect the  
184 combination effect range, ratios  $\frac{1}{CI}$  were calculated.

### 185 **2.8.2 Independent action concept**

186 The independent action (IA) concept was used as described by Fouquier and Guedj (2015). This  
187 method established by Bliss (1939) relies on the hypothesis that a combined effect can be calculated  
188 from the responses of the individual mixture components, assuming that each one acts independently  
189 without interfering with the others (different sites of action). In our study, for binary phycotoxin  
190 combinations, the predicted mixture effect values were calculated as follows:

$$191 \quad \begin{aligned} & Mix(A + B)predicted\ value \\ & = (mean\ value\ A + mean\ value\ B) - (mean\ value\ A \times mean\ value\ B) \end{aligned}$$

193

194 The CI were calculated as indicated by Fouquier and Guedj (2015):

$$195 \quad CI = \frac{Mix(A + B)predicted\ value}{Mix(A + B)measured\ value}$$

196 To establish the predictions, the raw data of ROS production, IL-8 release and  $\gamma$ -H2AX  
197 phosphorylation, originally expressed as fold change compared to the respective solvent control, were  
198 processed to obtain data suitable for IA analysis, i.e. comprised between 0 and 1. For each endpoint,  
199 the condition among the phycotoxins tested individually and the binary mixture showing the highest  
200 effect was attributed the value of 1 (Amax). All other conditions were then normalized to the Amax.  
201 This data processing was described previously by Alassane-Kpembé et al. (2016) and allows assessing  
202 combined effects for endpoints other than cell viability. The raw data of cell viability were first  
203 divided by 100 to get data comprised between 0 and 1. Cell viability values superior to 100 were set to  
204 1. Cell viability CI values were calculated as described for TA.

### 205 **3. Results**

#### 206 **3.1 Toxic effects following OA/PTX-2 mixtures treatment in Caco-2 cells**

##### 207 ***3.1.1 PTX-2 exacerbates the cytotoxicity of OA in Caco-2 cells***

208 PTX-2 alone was not toxic for Caco-2 cells, whereas OA showed concentration-dependent toxicity  
209 ( $IC_{50} = 331$  nM) (Fig. 1a). The binary OA/PTX-2 mixture induced strong cytotoxicity in Caco-2 cells,  
210 with a tremendous decrease of cells number (80% for the condition D) (Fig. 1a), indicating that the  
211 addition of PTX-2 increased the cytotoxicity of OA.

##### 212 ***3.1.2 PTX-2 decreases ROS production induced by OA***

213 After a 24 h treatment, OA not-statistically increased ROS production while PTX-2 had no effect (Fig.  
214 1b). We observed that low and intermediate concentrations of OA/PTX-2 (conditions B and C)  
215 reduced the level of ROS production compared to that induced by OA alone (Fig. 1b).

##### 216 ***3.1.3 PTX-2 decreases IL-8 release induced by OA only at low concentrations***

217 Only OA induced IL-8 release in Caco-2 cells (conditions B to E) (Fig. 1c). For low concentrations the  
218 OA/PTX-2 mixture resulted in a reduction of IL-8 release compared to that induced by OA alone,  
219 which was statistically significant for 37.5/12.5 nM (condition B). PTX-2 did not decrease IL-8  
220 production induced by OA at higher concentrations (Fig. 1c).

##### 221 ***3.1.3 PTX-2 decreases $\gamma$ -H2AX phosphorylation induced by OA at low concentrations***

222 PTX-2 alone slightly induced the phosphorylation of  $\gamma$ -H2AX (1.8-fold, not statistically significant)  
223 whereas OA concentration-dependently induced the phosphorylation of  $\gamma$ -H2AX even at low  
224 concentration (37.5 nM condition B, or higher) (Fig. 1d). For 37.5/12.5 nM (condition B), the mixture  
225 resulted in a lower phosphorylation of  $\gamma$ -H2AX compared to that induced by OA alone (Fig. 1d). This  
226 mixture effect is also illustrated by the immunostaining in Fig. 2. No data are provided for the three  
227 highest concentrations due to the high cytotoxicity that prevents from a reliable measurement of DNA  
228 damage.

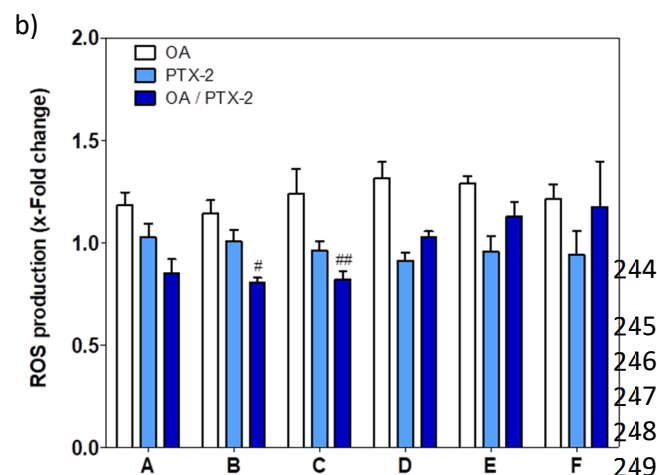
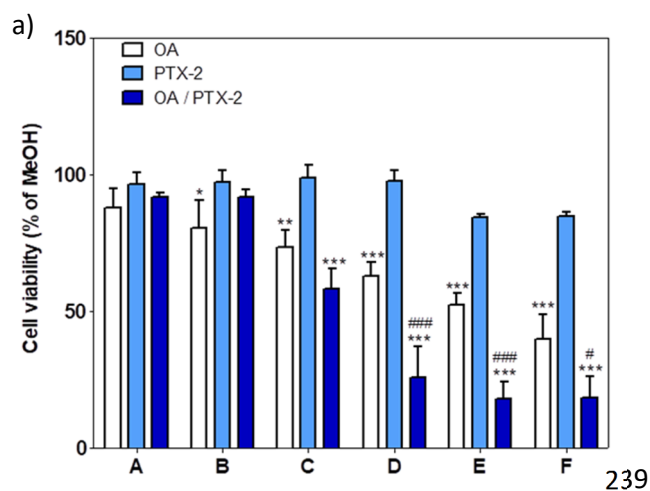
229

230

231

232

233



nM	solo		mixtures
	OA	PTX-2	OA/PTX-2
A	18.75	6.25	18.75/6.25
B	37.5	12.5	37.5/12.5
C	75	25	75/25
D	150	50	150/50
E	300	100	300/100
F	600	200	600/200

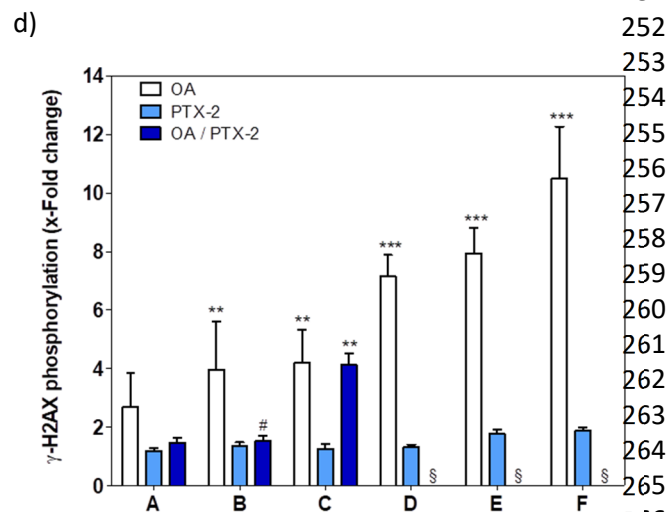
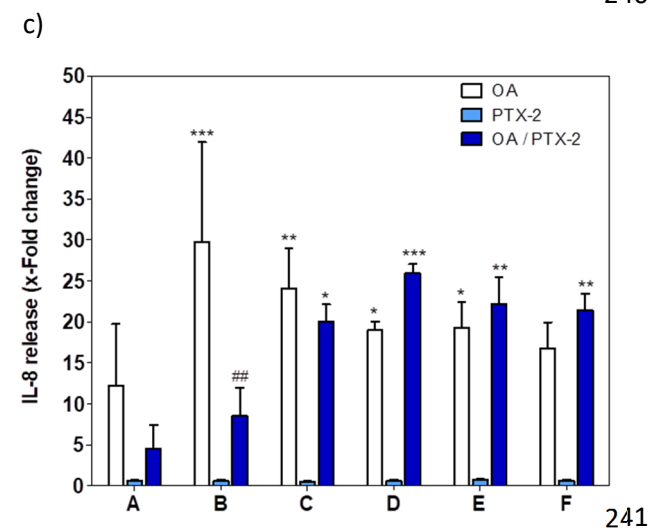


**Fig. 1** Effects of OA/PTX-2 mixtures on a panel of toxicity endpoints in differentiated Caco-2 cells. Cells were pre-treated with the ROS probe DCFH-DA (25  $\mu$ M) for 30 min before incubation with the toxin(s) for 24 h. After fluorometric measurement of ROS production, cell culture supernatant was collected for the quantification of IL-8 release, while cells were fixed for DAPI and  $\gamma$ -H2AX immunostaining: (a) cell viability, (b) ROS production, (c) IL-8 release and (d) phosphorylation of  $\gamma$ -H2AX are shown.  $\text{KBrO}_3$  (500  $\mu$ M) and  $\text{TNF}\alpha$  (20 ng/ml) were used as positive controls.  $\text{KBrO}_3$  increased ROS production by 1.5-fold and induced the phosphorylation of  $\gamma$ -H2AX by 2.7-fold.  $\text{TNF}\alpha$  failed to induce IL-8 release. Results were obtained from three independent experiments. Data represents means  $\pm$  SEM of fold change compared to solvent control. \*, \*\*, \*\*\* and #, ##, ### indicate statistical significance between toxin and solvent control or OA and mixture respectively ( $p < 0.05$ ,  $p < 0.01$ ,  $p < 0.001$  respectively) after two-way ANOVA followed by Bonferroni's post-hoc test. §: no data are provided due to high cytotoxicity that prevents from a reliable measurement of DNA damage.

234

235

236

237

238

239

240

241

242

243

244

245

246

247

248

249

250

251

252

253

254

255

256

257

258

259

260

261

262

263

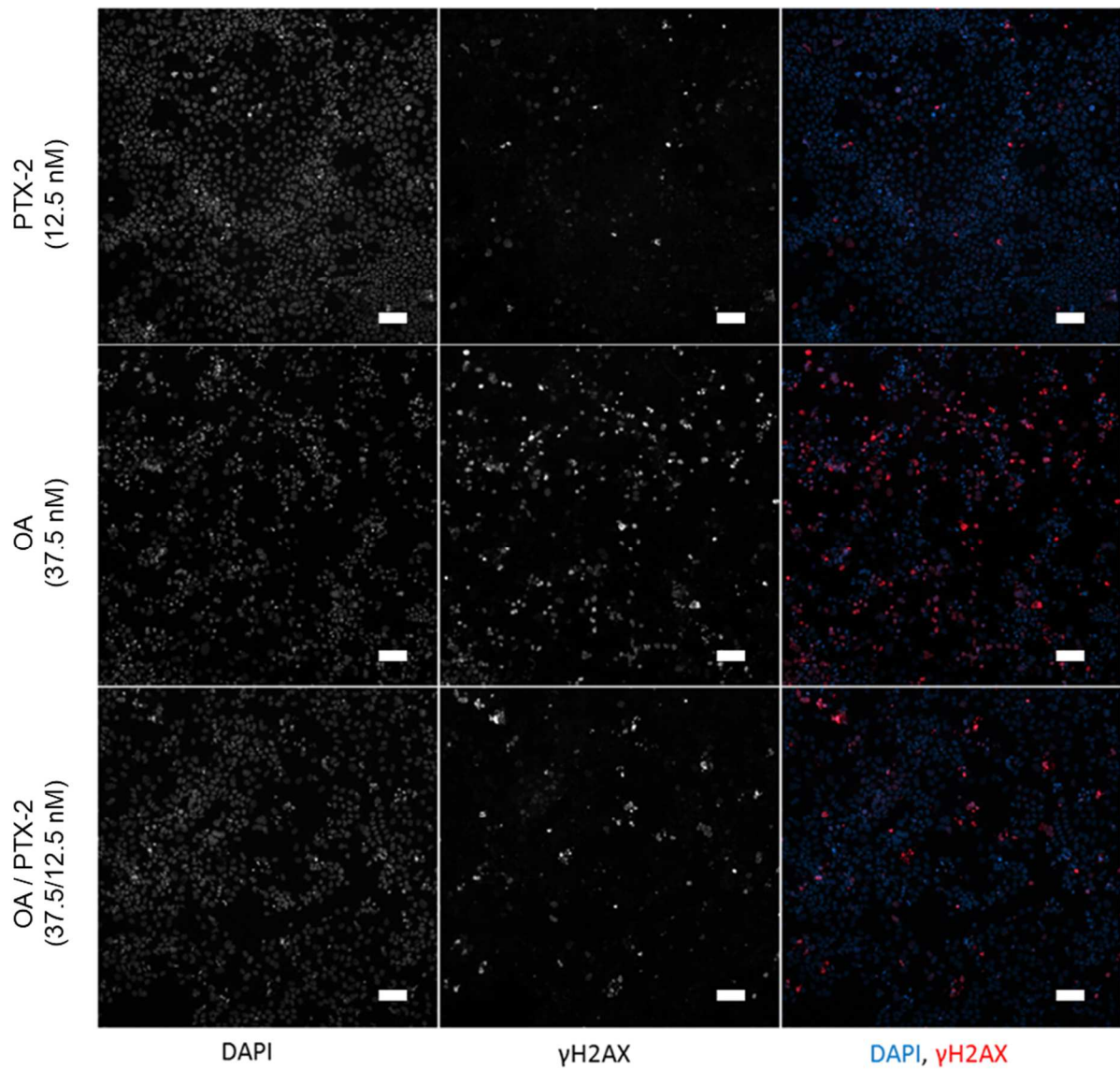
264

265

266

267

268



269

270 **Fig. 2** Representative images (10X magnification) of DNA damage induced by OA/PTX-2 mixtures.  
 271 Cells were incubated with toxins for 24 h and labeled with antibodies against  $\gamma$ -H2AX. The nuclei  
 272 were stained with DAPI and images were captured with an Arrayscan VTi. White bar = 100  $\mu$ m.

273

274

275

276

277

278

279 **3.2 Toxic effects following OA/SPX-1 mixtures treatment in Caco-2 cells**

280 **3.2.1 SPX-1 reduces the cytotoxicity effect of OA in Caco-2 cells at low concentrations**

281 SPX-1 was not toxic for Caco-2 cells in the tested range concentration. In mixture condition, a lower  
282 toxicity was depicted for low and intermediate concentrations (conditions B and C) even if not  
283 statistically significant (Fig. 3a).

284 **3.2.2 SPX-1 decreases ROS production induced by OA**

285 Whereas SPX-1 failed to induce ROS production, we observed that low and intermediate  
286 concentrations of OA/SPX-1 (conditions A, C and D) reduced the level of ROS production compared  
287 to that induced by OA alone (Fig. 3b).

288 **3.2.3 SPX-1 decreases IL-8 release induced by OA only at low concentrations**

289 SPX-1 did not induce the release of IL-8. For low concentrations the OA/SPX-1 mixture resulted in a  
290 reduction of IL-8 release compared to that induced by OA alone, which was statistically significant for  
291 37.5/12.5 nM (condition B). SPX-1 did not decrease IL-8 production induced by OA at higher  
292 concentrations (Fig. 3c).

293 **3.2.4 SPX-1 decreases  $\gamma$ -H2AX phosphorylation induced by OA at low concentrations**

294 No induction of  $\gamma$ -H2AX phosphorylation was observed after treatment with SPX-1. For 37.5/12.5 and  
295 600/200 nM (conditions B and F), the OA/SPX-1 mixture resulted in a reduced phosphorylation of  $\gamma$ -  
296 H2AX compared to that induced by OA alone (Fig. 1d). This mixture effect is also illustrated by the  
297 immunostaining in Fig. 4.

298

299

300

301

302

303

304

305

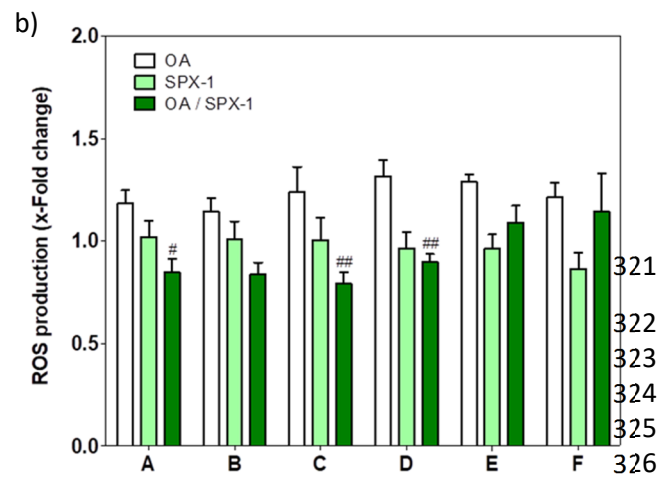
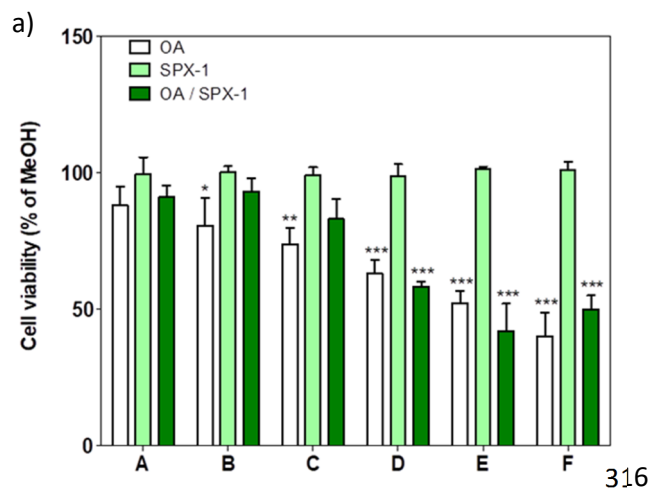
306

307

308

309

310



nM	solo		mixtures
	OA	SPX-1	OA/SPX-1
A	18.75	2.1	18.75/2.1
B	37.5	4.2	37.5/4.2
C	75	8.3	75/8.3
D	150	16.7	150/16.7
E	300	33.4	300/33.4
F	600	66.7	600/66.7

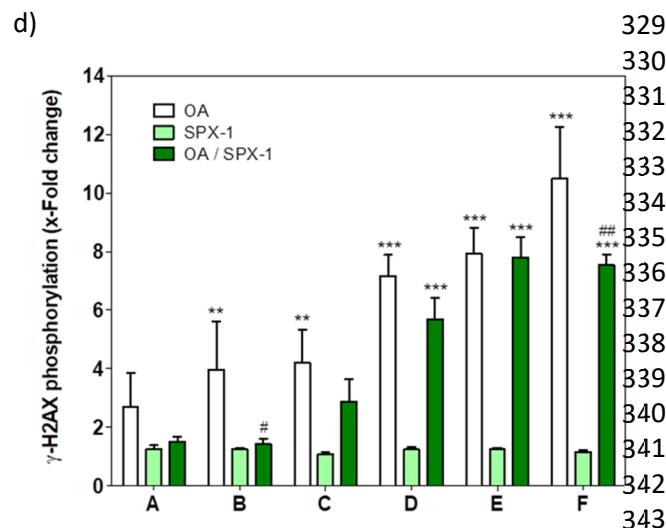
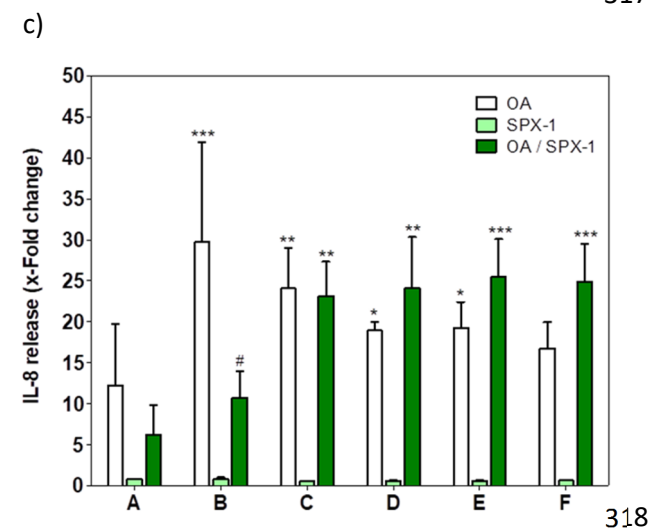


**Fig. 3** Effects of OA/SPX-1 mixtures on a panel of toxicity endpoints in differentiated Caco-2 cells. Cells were pre-treated with the ROS probe DCFH-DA (25  $\mu$ M) for 30 min before incubation with the toxin(s) for 24 h. After fluorometric measurement of ROS production, cell culture supernatant was collected for the quantification of IL-8 release, while cells were fixed for DAPI and  $\gamma$ -H2AX immunostaining: (a) cell viability, (b) ROS production, (c) IL-8 release and (d) phosphorylation of  $\gamma$ -H2AX are shown.  $\text{KBrO}_3$  (500  $\mu$ M) and  $\text{TnF}\alpha$  (20 ng/ml) were used as positive controls.  $\text{KBrO}_3$  increased ROS production by 1.5-fold and induced the phosphorylation of  $\gamma$ -H2AX by 2.7-fold.  $\text{TnF}\alpha$  failed to induce IL-8 release. Results were obtained from three independent experiments. Data represents means  $\pm$  SEM of fold change compared to solvent control. \*, \*\*, \*\*\* and #, ## indicate statistical significance between toxin and solvent control or OA and mixture respectively ( $p < 0.05$ ,  $p < 0.01$ ,  $p < 0.001$  respectively) after two-way ANOVA followed by Bonferroni's post-hoc test.

311

312

313

314

315

316

317

318

319

320

321

322

323

324

325

326

327

328

329

330

331

332

333

334

335

336

337

338

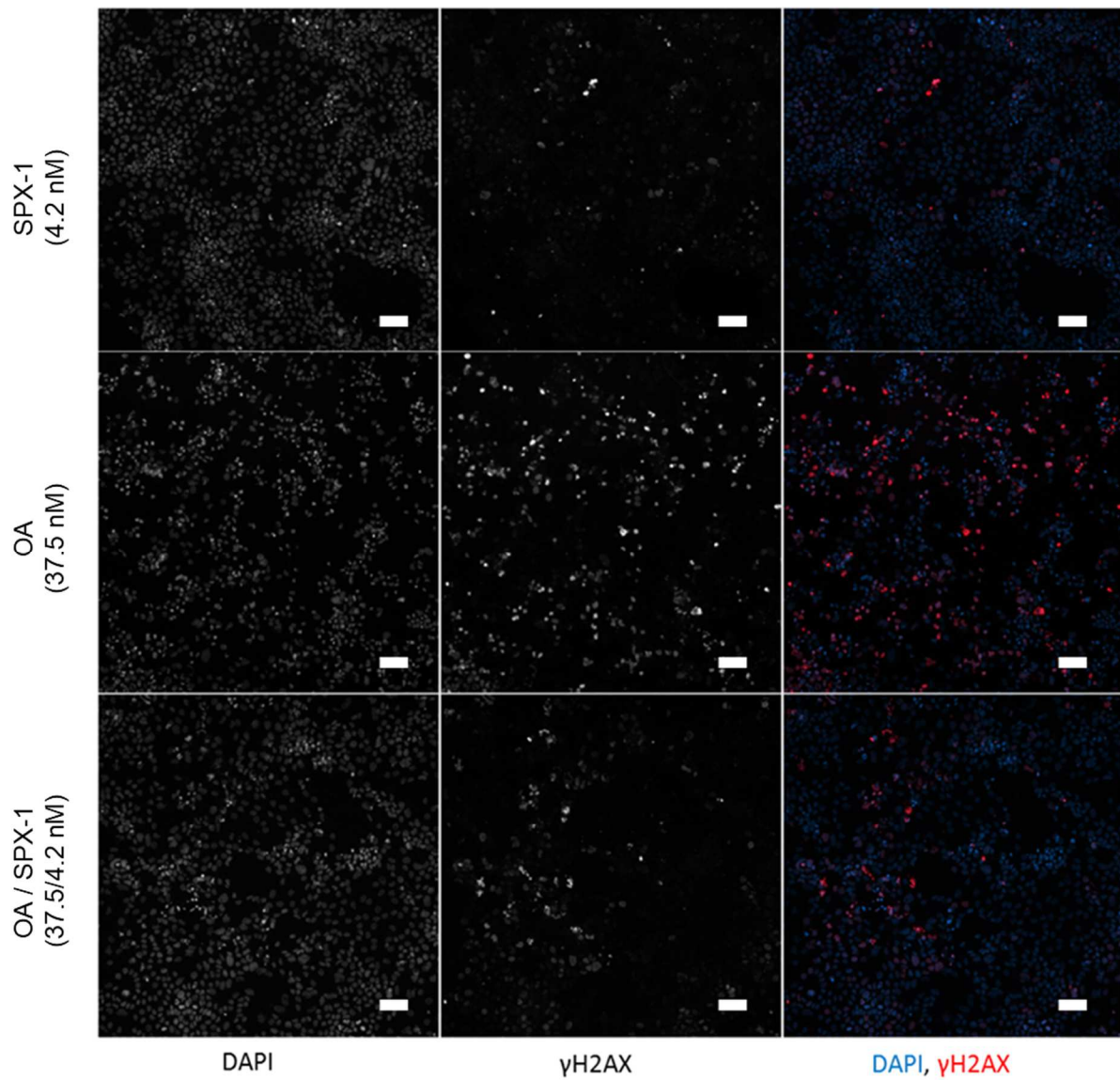
339

340

341

342

343



344

345 **Fig. 4** Representative images (10X magnification) of DNA damage induced by OA/SPX-1 mixtures.  
 346 Cells were incubated with toxins for 24 h and labeled with antibodies against  $\gamma$ -H2AX. The nuclei  
 347 were stained with DAPI and images were captured with an Arrayscan VTi. White bar = 100  $\mu$ m.

348

349

350

351

352

353

354 **3.3 Toxic effects following OA/YTX mixtures treatment in Caco-2 cells**

355 ***3.3.1 YTX reduces the cytotoxicity effect of OA in Caco-2 cells at low concentrations***

356 YTX was not toxic for Caco-2 cells in the tested range concentration. In mixture condition, a lower  
357 toxicity was depicted for low and intermediate concentrations (conditions A and B) even if not  
358 statistically significant (Fig. 5a).

359 ***3.3.2 YTX decreases ROS production induced by OA***

360 Whereas YTX failed to induce ROS production, we observed that low and intermediate concentrations  
361 of OA/YTX (conditions A and C) reduced the level of ROS production compared to that induced by  
362 OA alone.

363 ***3.3.3 YTX increases IL-8 release induced by OA at high concentrations***

364 If YTX failed to induce IL-8 release in Caco-2 cells, the mixtures with a high concentration of YTX  
365 showed an increase of IL-8 release compared to that induced by OA alone (conditions D and F) (Fig.  
366 5c).

367 ***3.3.4 YTX decreases  $\gamma$ -H2AX phosphorylation induced by OA at low concentrations***

368 No induction of  $\gamma$ -H2AX phosphorylation was observed after treatment with YTX. Similarly to what  
369 was observed for the OA/SPX-1 mixture, for 37.5/12.5 and 600/200 nM (conditions B and F), the  
370 OA/YTX mixture resulted in a reduced phosphorylation of  $\gamma$ -H2AX compared to that induced by OA  
371 alone (Fig. 1d). This mixture effect is also illustrated by the immunostaining in Fig. 6.

372

373

374

375

376

377

378

379

380

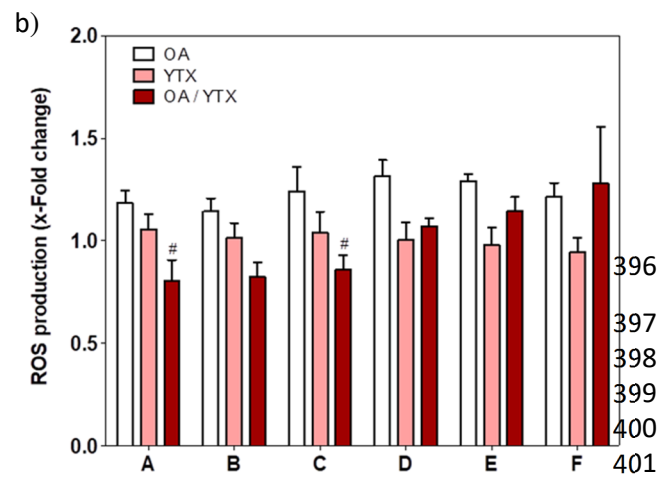
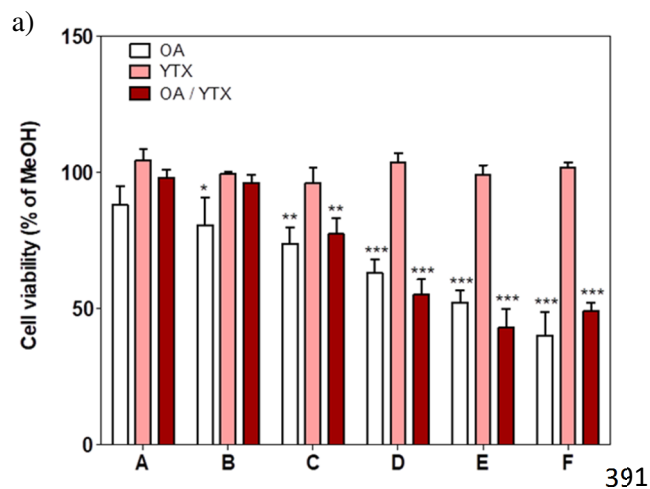
381

382

383

384

385



nM	solo		mixtures
	OA	YTX	OA/YTX
A	18.75	6.25	18.75/6.25
B	37.5	12.5	37.5/12.5
C	75	25	75/25
D	150	50	150/50
E	300	100	300/100
F	600	200	600/200

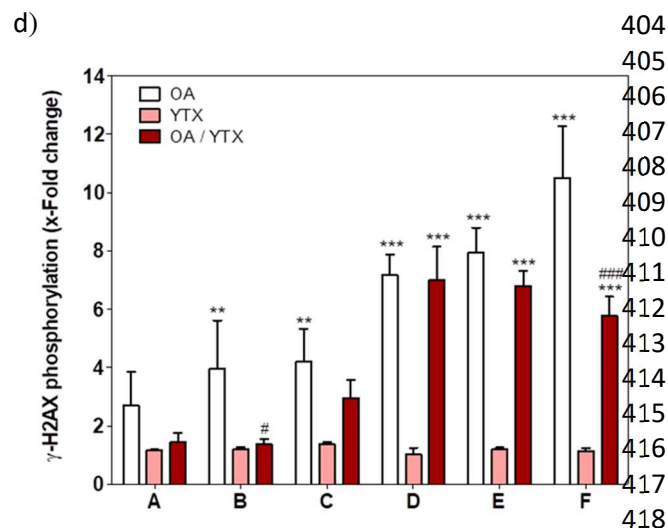
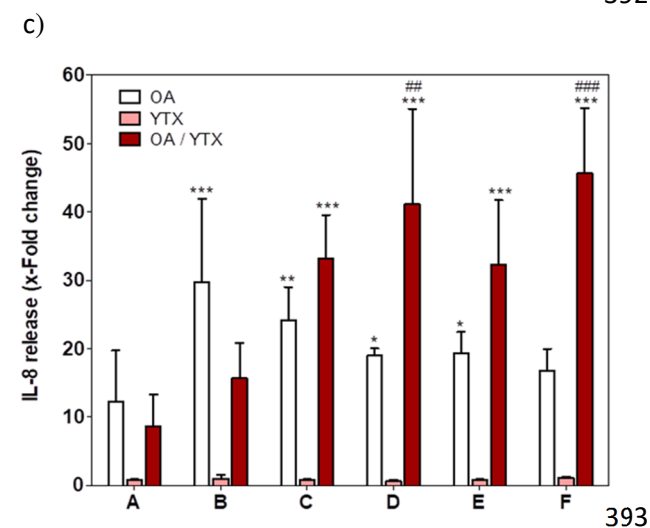


**Fig. 5** Effects of OA/YTX mixtures on a panel of toxicity endpoints in differentiated Caco-2 cells. Cells were pre-treated with the ROS probe DCFH-DA (25  $\mu$ M) for 30 min before incubation with the toxin(s) for 24 h. After fluorometric measurement of ROS production, cell culture supernatant was collected for the quantification of IL-8 release, while cells were fixed for DAPI and  $\gamma$ -H2AX immunostaining: (a) cell viability, (b) ROS production, (c) IL-8 release and (d) phosphorylation of  $\gamma$ -H2AX are shown. KBrO<sub>3</sub> (500  $\mu$ M) and TnF $\alpha$  (20 ng/ml) were used as positive controls. KBrO<sub>3</sub> increased ROS production by 1.5-fold and induced the phosphorylation of  $\gamma$ -H2AX by 2.7-fold. TNF $\alpha$  failed to induce IL-8 release. Results were obtained from three independent experiments. Data represents means  $\pm$  SEM of fold change compared to solvent control. \*, \*\*, \*\*\* and #, ##, ### indicate statistical significance between toxin and solvent control or OA and mixture respectively ( $p < 0.05$ ,  $p < 0.01$ ,  $p < 0.001$  respectively) after two-way ANOVA followed by Bonferroni's post-hoc test.

386

387

388

389

390

391

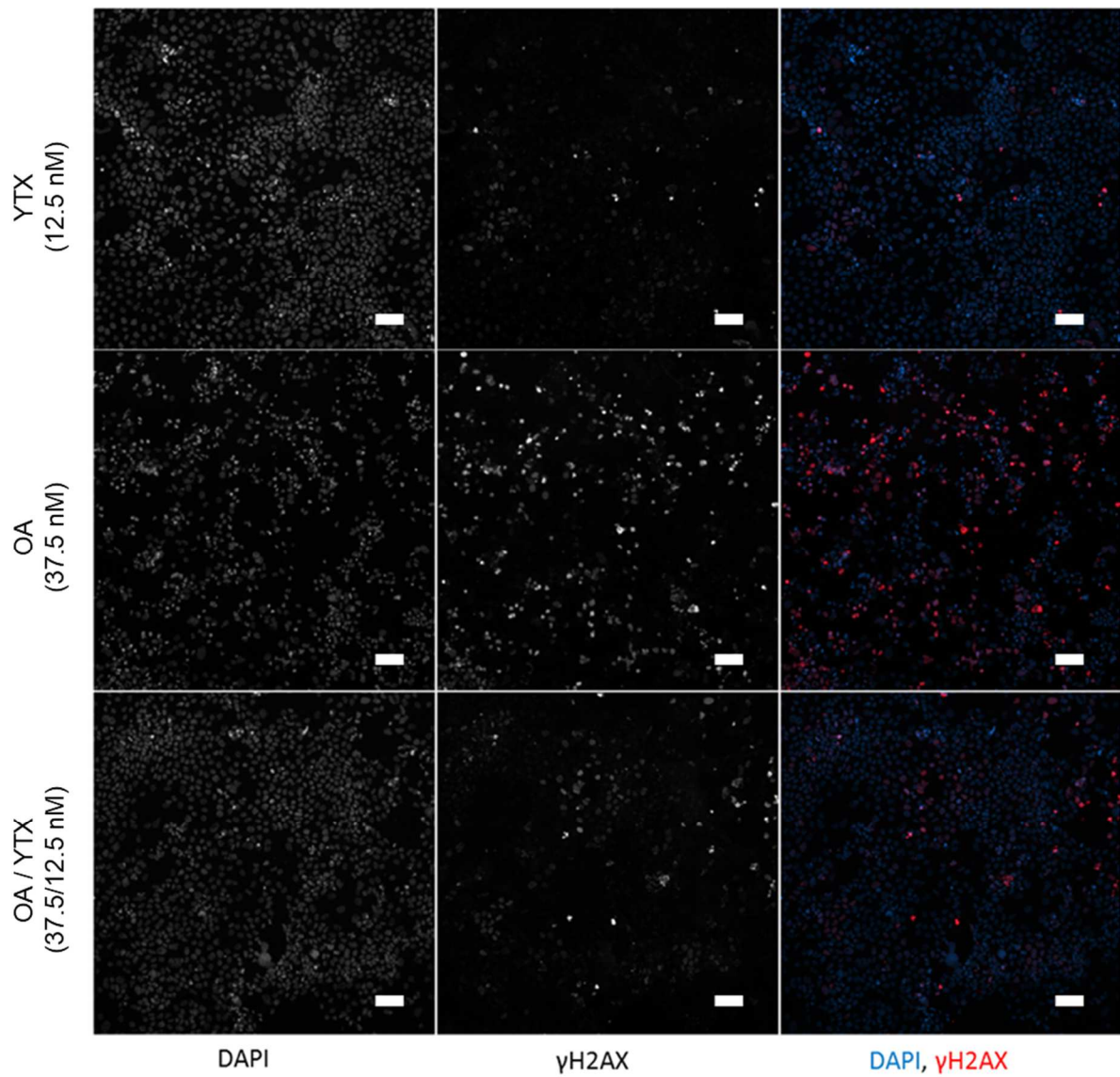
392

393

394

395

419



420

421 **Fig. 6** Representative images (10X magnification) of DNA damage induced by OA/YTX mixtures.  
 422 Cells were incubated with toxins for 24 h and labeled with antibodies against  $\gamma$ -H2AX. The nuclei  
 423 were stained with DAPI and images were captured with an Arrayscan VTi. White bar = 100  $\mu$ m.

424

425

426

427

428

429

430 **3.4 Predictions of mixture effects using the theoretical additivity (TA) method and the**  
431 **independent action (IA) concept**

432 **3.4.1 OA/PTX-2 mixtures treatment on Caco-2 cells**

433 Regarding cytotoxicity, TA model predicted additivity or antagonism for the two low concentrations  
434 while synergism occurred at higher concentrations except for the highest concentration where  
435 additivity was shown (Fig. 7a). IA model predicted additivity for the two low concentrations and  
436 synergism at higher concentrations. Using IA model, antagonism was observed for all concentrations  
437 towards ROS production while TA predicted additivity for the two highest concentrations. For  $\gamma$ -  
438 H2AX phosphorylation, no predictions at the three highest concentrations were made due to the high  
439 cytotoxicity that prevents from a reliable measurement of DNA damage. Both models gave similar  
440 predictions of antagonism for A and B conditions while C condition showed additivity. Antagonism  
441 towards IL-8 release was obtained for low concentrations, compared to slight synergism or additivity  
442 at higher concentrations with both models.

443 **3.4.2 OA/SPX-1 mixtures treatment on Caco-2 cells**

444 Regarding cytotoxicity, no clear tendency emerges but additivity seems to be the main effect occurring  
445 using TA model (Fig. 7b). IA model predicted additivity for the two low concentrations and synergism  
446 at higher concentrations. For IL-8 release, all kinds of effects were observed from antagonism at the  
447 lowest concentrations, to additivity or synergism at the intermediate and highest concentrations  
448 respectively. Using IA model, antagonism was observed for all concentrations towards ROS  
449 production while TA predicted additivity for the highest concentration. For  $\gamma$ -H2AX phosphorylation,  
450 both models predicted antagonism except for E condition where additivity was described.

451 **3.4.3 OA/YTX mixtures treatment on Caco-2 cells**

452 Regarding cytotoxicity, no clear tendency emerges but additivity seems to be the main effect occurring  
453 using TA model (Fig. 7c). IA model predicted additivity for the two low concentrations and synergism  
454 at higher concentrations. ROS measurement and  $\gamma$ -H2AX phosphorylation showed antagonism for  
455 almost all concentrations, additivity being sometimes described (e.g D condition for  $\gamma$ -H2AX  
456 phosphorylation or F condition for ROS with TA). Antagonism towards IL-8 release was obtained for  
457 low concentrations, compared to synergism at higher concentrations.

458

459

460

461

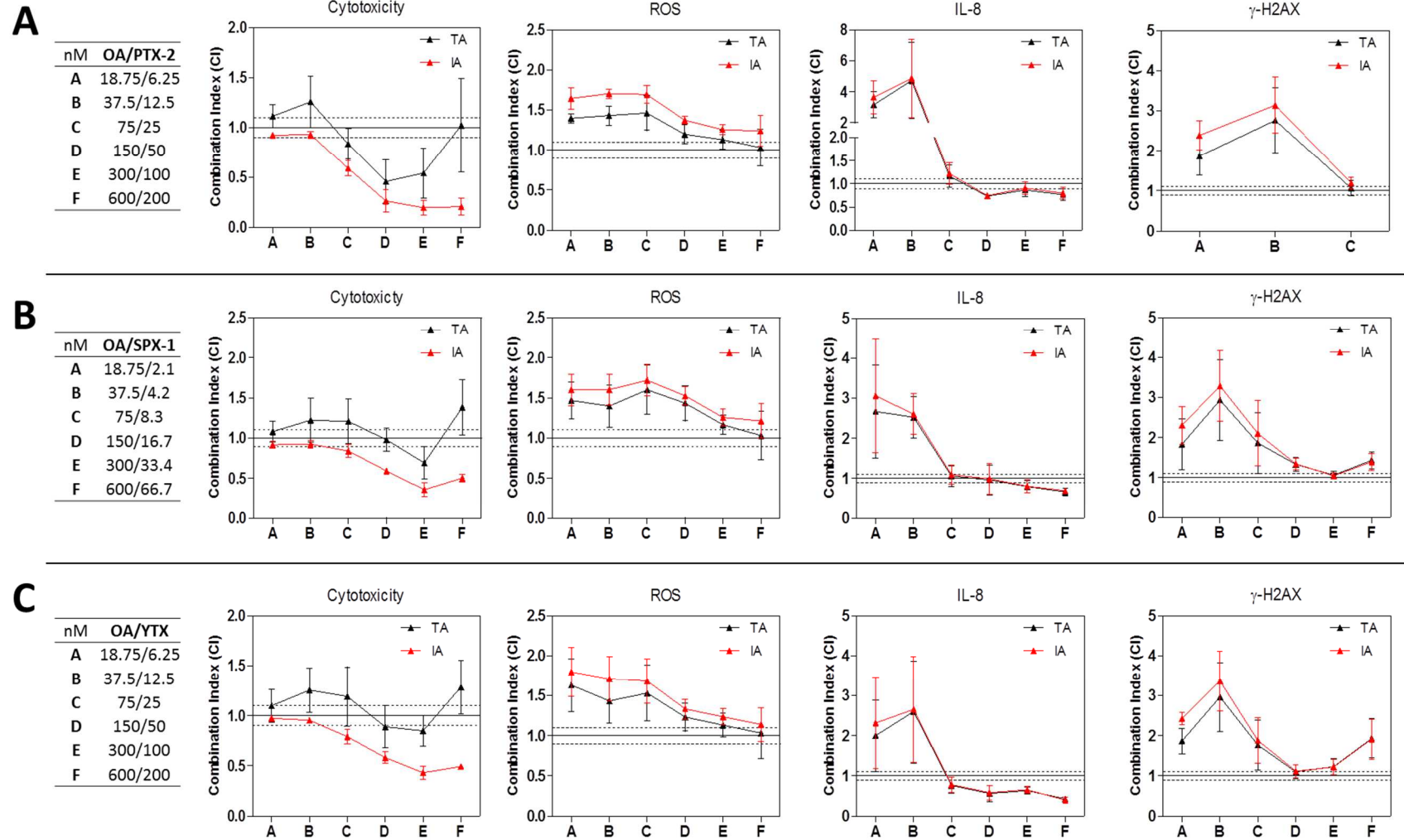
462

463

464

465

466 **Fig. 7** Analysis of mixtures using the theoretical additivity (TA) method and the independent action (IA) concept on a panel of toxicity endpoints in differentiated  
 467 Caco-2 cells. CI < 0.9,  $0.9 \leq CI \leq 1.1$  and  $CI > 1.1$  indicate respectively synergism, additive effect and antagonism. Data represents means  $\pm$  SEM from three  
 468 independent experiments. Dashed lines indicate lower and upper limits of additivity.



469

#### 470 4. Discussion (1500 words)

471 In this study, we investigated the effects of binary mixtures of lipophilic phycotoxins on a variety of  
472 toxicity endpoints in a human intestinal cell model. The mixture compositions and ratios were selected  
473 according to a review of the literature on phycotoxin mixtures (Alarcan et al., 2018). Three main  
474 mixtures were tested, all of them featuring OA as the major constituent and reflecting realistic  
475 exposure scenarios. Irrespective of the phycotoxin combined with OA, the effects observed were,  
476 according to the chosen mathematical approach, mainly antagonistic at low concentrations and, in a  
477 few cases, synergistic at higher concentrations.

478 When investigating mixture effects, the choice of endpoints is a main concern. A specific endpoint can  
479 be easily selected when the compounds share a common mechanism of action. In our case, the toxins  
480 tested have different mechanisms of action, and therefore a single relevant common endpoint can  
481 hardly be chosen. Therefore, we designed a multi-parametric approach for an integrative analysis of  
482 toxic responses. To this end, we selected different endpoints among widely studied toxicological  
483 pathways.

484 Our study revealed that OA was cytotoxic, induced DNA strand-breaks and triggered the release of IL-  
485 8 from differentiated Caco-2 cells, similar to the effects reported with proliferative Caco-2 cells by  
486 Ferron et al. (2014). These effects correspond to observations from *in vivo* studies in rodents that  
487 reported erosion of the epithelium and release of inflammatory mediators following oral exposure to  
488 OA (Aune et al., 2012, Tubaro et al., 2003, Ito et al., 2002). PTX-2 did not affect Caco-2 cell viability  
489 and only slightly induced DNA strand-breaks at the highest concentrations. SPX-1 and YTX did not  
490 induce any effect on all tested endpoints. The absence of toxic effects correlates well with *in vivo*  
491 studies in rodents that did not report particular effects on the gastro-intestinal tract following oral  
492 exposure to these toxins (Aune et al., 2002, Tubaro et al., 2003, Munday et al., 2012). Irrespective of  
493 the phycotoxin, no ROS production was detected. However we cannot exclude that ROS might have  
494 been produced earlier and were already neutralized after 24h due to protective cellular anti-oxidant  
495 systems

496 Two different conceptual approaches were employed to assess the combined effects of phycotoxins in  
497 mixture. The TA method and IA concept offer the advantage to be easy to handle, fast and applicable  
498 to all kind of data. We showed that under the present settings and parameters additivity was rarely  
499 predicted irrespective of the mixture and the endpoint tested, meaning that the phycotoxins tested  
500 might be able to interact and modulate their toxic effects. Therefore, in absence of additivity, the two  
501 approaches are not appropriate to predict the toxicity of phycotoxin mixtures. In this case, the  
502 combined effects of phycotoxins must be determined from experimental data. Besides, caution needs  
503 to be taken with mixture simulations. For instance, in our study, IA analysis revealed strong synergism  
504 towards cell viability for OA/SPX-1 and OA/YTX (Figure 7) whereas raw data revealed only a slight  
505 or no increase of toxicity with mixtures (Figures 3a and 5a). It is noteworthy that a general assumption  
506 of additivity may not be reliable since OA is believed to target different serine/threonine protein  
507 phosphatases (PP) depending on its concentration: the estimated  $IC_{50}$  for PP1 is 10-100 nM, while  
508 being 100-fold inferior for PP2A (0.1-1 nM) (Cruz et al., 2013). Indeed, Gehringer (2004) suggested  
509 that the PP inhibitors microcystin-LR and OA showed a dualistic response by inducing different  
510 cellular effects depending on the concentration used, and therefore on the PP isoform inhibited.

511 Since few years, the Chou-Talalay method (Chou and Talalay 1984) has received considerable interest  
512 in the context of food contaminant mixtures (Alassane-Kpembi et al., 2016, Ferron et al., 2016, Smith  
513 et al., 2017, Karri et al., 2018). This easy-to-use method is a powerful tool which offers a quantitative  
514 definition for additivity and the type of interaction (synergism or antagonism) in chemical mixtures.

515 Based on the median-effect equation, it requires that each compound alone and in mixtures follows the  
516 principle of the mass-action law (e.g.,  $r > 0.95$ ). Therefore the method is not suitable when one drug  
517 does not exert any effect (Chou, 2006). In our study, most endpoints were not affected by at least one  
518 of the toxins, and consequently the Chou-Talalay method would not be appropriate.

519 Our study revealed that only OA provoked IL-8 release. However, we observed a greater effect at high  
520 concentrations with the OA/YTX mixture, meaning that YTX may potentiate the OA response. A  
521 similar hypothesis can be deduced for the cytotoxicity of OA/PTX-2 mixture. However, confirmation  
522 of such observations through a mathematical model was not possible since none exists for testing  
523 potentiation.

524 Irrespective of the toxin, mixtures with OA always resulted in a diminished toxic response at low  
525 concentrations (ROS production, IL-8 release and H2AX phosphorylation), whereas a higher toxic  
526 response was observed for some endpoints at high concentrations. A diminished ROS production  
527 might be linked to a diminished DNA damage response, as it is known that ROS can cause DNA  
528 breaks (Moloney and Cotter 2018). Moreover, many studies have shown that the inhibition of ROS by  
529 the use of a scavenger leads to a lowered DNA damage response (Luo et al., 2013, He et al., 2014,  
530 Chen et al., 2018). ROS have been shown to activate NF- $\kappa$ B, a transcription factor responsible for IL-8  
531 regulation (Kurata et al., 1996, Pahl 1999, Oeckinghaus and Ghosh 2009). Since all these endpoints  
532 are interconnected, the systematic decrease of responses that was observed with mixtures at low  
533 concentrations in our experiments appears consistent. The protective mechanisms behind this might  
534 relate to changes in the absorption and/or the metabolism of toxins in the mixtures. For instance, OA  
535 was previously found to interact with regulatory nuclear receptors such as PXR (Fidler et al., 2012;  
536 Ferron et al., 2016), which regulate the expression of some cytochrome P450 enzymes (Wang et al.,  
537 2012). PTX-2 is believed to interact with the AhR since it induces CYP1A protein in hepatic cells  
538 (Alarcan et al., 2017). Moreover, OA, PTX-2 and SPX-1 have been shown to be metabolized through  
539 cytochromes P450 (Guo et al., 2010, Hui et al., 2012, Kittler et al., 2014, Alarcan et al., 2017).  
540 Therefore, at low concentrations, mixtures might induce CYP activity and efflux transporter  
541 expression, resulting in higher detoxification/excretion of toxins and thus decreased toxic effects. In  
542 favor of this hypothesis, the few oral *in vivo* studies conducted with phycotoxin mixtures showed a  
543 reduced uptake of toxins (Alarcan et al., 2018). As PTX-2, YTX and SPX-1 have different  
544 mechanisms of action, we assume that the potential protective effect, as suggested by the mathematical  
545 evaluation of our *in vitro* data, did not result from the disturbance of a single specific OA-dependent  
546 pathway. The strong synergistic effect observed for the cytotoxicity of the OA/PTX-2 mixture at  
547 higher concentrations may imply cytoskeleton homeostasis. Indeed, even if no cytotoxicity following  
548 treatment with PTX-2 has been observed, the toxin clearly disrupts the actin network (Alligham et al.,  
549 2007). OA has also been demonstrated to change the organization of the actin network (Fiorentini et  
550 al., 1996; Vale and Botana 2008). Disruption of the cytoskeleton has been shown to be a starting event  
551 leading to an induction of pro-apoptotic effectors (e.g caspase-3 activation) (Yamazaki et al., 2000,  
552 White et al., 2001, Martin and Leder 2001, Kulms et al., 2002). Therefore, the disruption of the actin  
553 cytoskeleton by both, PTX-2 and OA, may explain the possible synergism observed with the mixture.

554 Toxins of the OA group and of the PTX group share a common European regulatory limit but their  
555 behavior in mixtures is largely unknown. Results from this study suggest a possible synergistic  
556 cytotoxic effect at moderate and high concentrations in Caco-2 cells, a model mimicking the human  
557 intestinal barrier. Further research is needed to confirm the present findings and to judge on their  
558 relevance for humans exposed to phycotoxins via the diet.

## 559 **5. Conclusions**

560 In this study, we assessed the *in vitro* effects of binary mixtures of lipophilic phycotoxins on human  
561 intestinal cells towards multiple toxicity endpoints. Mainly antagonistic effects were depicted at low  
562 concentrations and, in few cases, a strong synergism was detected at higher concentrations. These  
563 findings need to be confirmed with additional experiments and completed with *in vivo* studies to bring  
564 further evidence on the combined effects of lipophilic phycotoxins.

565 **Declarations of interest:** none

#### 566 **Authorship Contributions**

567 Participated in research design: Alarcan, Le Hégarat, Fessard, Hessel-Pras, Lampen

568 Conducted experiments: Alarcan, Barbé

569 Contributed new reagents or analytical tools:

570 Performed data analysis: Alarcan

571 Wrote or contributed to the writing of the manuscript: Alarcan, Le Hégarat, Kopp, Hessel-Pras,  
572 Braeuning, Lampen and Fessard

#### 573 **Funding information**

574 This work was financed by the French Agency for Food, Environmental and Occupational Health &  
575 Safety (ANSES) and by the German Federal Institute for Risk Assessment (BfR).

#### 576 **References**

577 Aune, T.; Sorby, R.; Yasumoto, T.; Ramstad, H.; Landsverk, T. Comparison of oral and  
578 intraperitoneal toxicity of yessotoxin towards mice. *Toxicon* 2002, 40, 77–82.

579 Aune T, Espenes A, Aasen JAB, Quilliam MA, Hess P, Larsen S. Study of possible combined toxic  
580 effects of azaspiracid-1 and okadaic acid in mice via the oral route. *Toxicon*. 2012 Oct;60(5):895–906.

581 Aasen JAB, Espenes A, Miles CO, Samdal IA, Hess P, Aune T. Combined oral toxicity of azaspiracid-  
582 1 and yessotoxin in female NMRI mice. *Toxicon*. 2011 May;57(6):909–17.

583 Alarcan J, Dubreil E, Huguet A, Hurtaud-Pessel D, Hessel-Pras S, Lampen A, Fessard V, Le Hegarat  
584 L. Metabolism of the Marine Phycotoxin PTX-2 and Its Effects on Hepatic Xenobiotic Metabolism:  
585 Activation of Nuclear Receptors and Modulation of the Phase I Cytochrome P450. *Toxins (Basel)*.  
586 2017 Jul 5;9(7).

587 Alassane-Kpembé I., Puel O., Pinton P., Cossalter A.M., Chou T.C., Oswald I.P. Co-exposure to low  
588 doses of the food contaminants deoxynivalenol and nivalenol has a synergistic inflammatory effect on  
589 intestinal explants. *Arch. Toxicol*. 2017;91:2677–2687.

590 Alassane-Kpembé I., Schatzmayr G., Taranu I., Marin D., Puel O., Oswald I.P. Mycotoxins co-  
591 contamination: Methodological aspects and biological relevance of combined toxicity studies. *Crit.*  
592 *Rev. Food Sci. Nutr*. 2017;57:3489–3507.

593 Alexander, J., Benford, D., Boobis, A., Ceccatelli, S., Cravedi, J.-P., Di, A., Domenico, D.D.,  
594 Dogliotti, E., Edler, L., Farmer, P., et al. (2009). Marine biotoxins in shellfish—Summary on regulated

595 marine biotoxins Scientific Opinion of the Panel on Contaminants in the Food Chain. EFSA J 1306, 1–  
596 23.

597 Allingham JS, Miles CO, Rayment I. A Structural Basis for Regulation of Actin Polymerization by  
598 Pectenotoxins. J Mol Biol. 2007 Aug;371(4):959–70.

599 Aráoz R, Ouanounou G, Iorga BI, Goudet A, Alili D, Amar M, et al. The Neurotoxic Effect of 13,19-  
600 Didesmethyl and 13-Desmethyl Spirolide C Phycotoxins Is Mainly Mediated by Nicotinic Rather  
601 Than Muscarinic Acetylcholine Receptors. Toxicol Sci. 2015 Sep;147(1):156–67.

602 Bliss CI. The toxicity of poisons applied jointly. Ann Appl Biol. 1939;26: 585–615.

603 Chen X, Song L, Hou Y, Li F. Reactive oxygen species induced by icaritin promote DNA strand  
604 breaks and apoptosis in human cervical cancer cells. Oncol Rep. 2018; 41: 765-778.

605 Chou TC, Talalay P. (1984). Quantitative analysis of dose-effect relationships: the combined effects of  
606 multiple drugs or enzyme inhibitors. Adv Enzyme Regul 22:27–5.

607 Chou TC. Theoretical basis, experimental design, and computerized simulation of synergism and  
608 antagonism in drug combination studies. Pharmacol Rev. 2006;58:621–681.

609 Cruz, P.G.; Norte, M.; Creus, A.H.; Fernández, J.J.; Daranas, A.H. Self-association of okadaic Acid:  
610 Structural and pharmacological significance. Mar. Drugs 2013, 11, 1866–1877.

611 Diogène G., Fessard V., Dubreuil A., Puiseux-Dao S. Comparative studies of the actin cytoskeleton  
612 response to maitotoxin and okadaic acid. Toxic. In Vitro. 1995; 9(1):1-10.

613 Ehlers A., Scholz J., These A., Hessel S., Preiss-Weigert A., Lampen A. Analysis of the passage of the  
614 marine biotoxin okadaic acid through an *in vitro* human gut barrier. Toxicology. 2011;279:196–202.

615 Fernández-Araujo A, Alfonso A, Vieytes MR, Botana LM. Key role of phosphodiesterase 4A  
616 (PDE4A) in autophagy triggered by yessotoxin. Toxicology. 2015 Mar;329:60–72.

617 Ferron, P.-J., Hogeveen, K., Fessard, V., and Hégarat, L. (2014). Comparative Analysis of the  
618 Cytotoxic Effects of Okadaic Acid-Group Toxins on Human Intestinal Cell Lines. Mar. Drugs 12,  
619 4616–4634.

620 Ferron, P.J., Hogeveen, K., De Sousa, G., Rahmani, R., Dubreuil, E., Fessard, V., and Le Hégarat, L.  
621 (2016). Modulation of CYP3A4 activity alters the cytotoxicity of lipophilic phycotoxins in human  
622 hepatic HepaRG cells. Toxicol. In Vitro 33, 136–146.

623 Ferron P-J, Dumazeau K, Beaulieu J-F, Le Hégarat L, Fessard V. Combined Effects of Lipophilic  
624 Phycotoxins (Okadaic Acid, Azapsiracid-1 and Yessotoxin) on Human Intestinal Cells Models.  
625 Toxins. 2016 Feb 19;8(2):50.

626 Fidler A.E., Holland P.T., Reschly E.J., Ekins S., Krasowski M.D. Activation of a tunicate (*Ciona*  
627 *intestinalis*) xenobiotic receptor orthologue by both natural toxins and synthetic toxicants. Toxicon.  
628 2012;59:365–372.

629 Fiorentini, C.; Matarrese, P.; Fattorossi, A.; Donelli, G. Okadaic acid induces changes in the  
630 organization of F-actin in intestinal cells. Toxicon 1996, 34, 937–945.

631 Fouquier, J., Guedj, M., 2015. Analysis of drug combinations: current methodological landscape.  
632 *Pharmacol. Res. Perspect.* 3.

633 Gehringer M.M. Microcystin-LR and okadaic acid-induced cellular effects: A dualistic response.  
634 *FEBS Lett.* 2004;557:1–8.

635 Guo, F.; An, T.; Rein, K.S. The algal hepatotoxin okadaic acid is a substrate for human cytochromes  
636 CYP3A4 and CYP3A5. *Toxicol* 2010, 55, 325–332.

637 He P. X., Zhang J., Che Y. S., He Q. J., Chen Y., Ding J. (2014). G226, a new  
638 epipolythiodioxopiperazine derivative, triggers DNA damage and apoptosis in human cancer cells in  
639 vitro via ROS generation. *Acta Pharmacol. Sin.* 35 1546–1555.

640 Hui JPM, Stuart Grossert J, Cutler MJ, Melanson JE. (2012). Strategic identification of in vitro  
641 metabolites of 13-desmethyl spirolide C using liquid chromatography/high-resolution mass  
642 spectrometry: Identification of in vitro metabolites of 13-desmethyl spirolide C. *Rapid Commun Mass*  
643 *Spectrom.* 26(3), 345–54.

644 Ito, E., Yasumoto, T., Takai, A., Imanishi, S., and Harada, K. (2002). Investigation of the distribution  
645 and excretion of okadaic acid in mice using immunostaining method. *Toxicol* 40, 159–165.

646 Ito, E., Suzuki, T., Oshima, Y., and Yasumoto, T. (2008). Studies of diarrhetic activity on  
647 pectenotoxin-6 in the mouse and rat. *Toxicol* 51, 707–716.

648 Karri V, Kumar V, Ramos D, Oliveira E, Schuhmacher M. An in vitro cytotoxic approach to assess  
649 the toxicity of heavy metals and their binary mixtures on hippocampal HT-22 cell line. *Toxicol Lett.*  
650 2018 Jan 5;282:25-36.

651 Kittler K, Fessard V, Maul R, Hurtaud-Pessel D. CYP3A4 activity reduces the cytotoxic effects of  
652 okadaic acid in HepaRG cells. *Arch Toxicol.* 2014;88(8):1519–1526.

653 Kulms D., Dussmann H., Poppelmann B., Stander S., Schwarz A., Schwarz T. Apoptosis induced by  
654 disruption of the actin cytoskeleton is mediated via activation of CD95 (FAS/APO-1) *Cell Death*  
655 *Differ.* 2002;9:598–608.

656 Kurata S, Matsumoto M, Tsuji Y, Nakajima H (1996) Lipopolysaccharide activates transcription of  
657 the hemoxygenase gene in mouse M1 cells through oxidative activation of nuclear factor kappa B.  
658 *Eur J Biochem.* 239: 566–571.

659 Loewe, S. and Muischnek, H. (1926) Ueber Kombinationswirkungen. *Naunyn-Schmiedeberg's*  
660 *Archives of Pharmacology*, 114, 313–326.

661 Luo H, Yang A, Schulte BA, Wargovich MJ, Wang GY. Resveratrol induces premature senescence in  
662 lung cancer cells via ROS-mediated DNA damage. *PLoS One.* 2013;8(3):e60065.

663 Martin SS, Leder P. Human MCF10A mammary epithelial cells undergo apoptosis following actin  
664 depolymerization that is independent of attachment and rescued by Bcl-2. *Mol Cell Biol.*  
665 2001;21(19):6529–6536.

666 Moloney JN, Cotter TG. ROS signalling in the biology of cancer. *Semin Cell Dev Biol.* 2018;80:50–  
667 64.

668 Munday R, Quilliam MA, LeBlanc P, Lewis N, Gallant P, Sperker SA, et al. Investigations into the  
669 Toxicology of Spirolides, a Group of Marine Phycotoxins. *Toxins*. 2011 Dec 30;4(12):1–14.

670 Oeckinghaus A, Ghosh S. The NF-kappaB family of transcription factors and its regulation. *Cold  
671 Spring Harb Perspect Biol*. 2009;1:a000034.

672 Pahl HL. Activators and target genes of Rel/NF-κB transcription factors. *Oncogene*. 1999;18:6853.

673 Rodríguez L, González V, Martínez A, Paz B, Lago J, Cordeiro V, et al. Occurrence of Lipophilic  
674 Marine Toxins in Shellfish from Galicia (NW of Spain) and Synergies among Them. *Mar Drugs*. 2015  
675 Mar 25;13(4):1666–87.

676 Sambuy Y, De Angelis I, Ranaldi G, Scarino ML, Stammati a, Zucco F. The Caco-2 cell line as a  
677 model of the intestinal barrier: influence of cell and culture-related factors on Caco-2 cell functional  
678 characteristics. *Cell Biol Toxicol*. (2005) 21:1–26.

679 Smith M.C., Hymery N., Troadec S., Pawtowski A., Coton E., Madec S. Hepatotoxicity of  
680 fusariotoxins, alone and in combination, towards the HepaRG human hepatocyte cell line. *Food Chem.  
681 Toxicol*. 2017;109:439–451.

682 Sosa S, Ardizzone M, Beltramo D, Vita F, Dell’Ovo V, Barreras A, et al. Repeated oral co-exposure to  
683 yessotoxin and okadaic acid: A short term toxicity study in mice. *Toxicol*. 2013 Dec;76:94–102.

684 Takai, A., Murata, M., Torigoe, K., Isobe, M., Mieskes, G., and Yasumoto, T. (1992). Inhibitory effect  
685 of okadaic acid derivatives on protein phosphatases. A study on structure-affinity relationship.  
686 *Biochem. J*. 284 ( Pt 2), 539–544.

687 Tubaro A, Sosa S, Carbonatto M, Altinier G, Vita F, Melato M, et al. Oral and intraperitoneal acute  
688 toxicity studies of yessotoxin and homoyessotoxins in mice. *Toxicol*. 2003;41(7):783–92.

689 Tubaro A, Dell’Ovo V, Sosa S, Florio C. Yessotoxins: A toxicological overview. *Toxicol*. 2010  
690 Aug;56(2):163–72.

691 Valdiglesias, V., Prego-Faraldo, M.V., Pásaro, E., Méndez, J., and Laffon, B. (2013). Okadaic acid:  
692 more than a diarrhetic toxin. *Mar. Drugs* 11, 4328–4349.

693 Vale C., Botana L.M. Marine toxins and the cytoskeleton: Okadaic acid and dinophysistoxins. *FEBS J*.  
694 2008;275:6060–6066.

695 Visciano P., Schirone M., Berti M., Milandri A., Tofalo R., Suzzi G. (2016). Marine biotoxins:  
696 occurrence, toxicity, regulatory limits and reference methods. *Front. Microbiol*. 7:1051.

697 Wang Y.M., Ong S.S., Chai S.C., Chen T. Role of CAR and PXR in xenobiotic sensing and  
698 metabolism. *Expert Opin. Drug Metab. Toxicol*. 2012;8:803–817.

699 Weber, F.; Freudinger, R.; Schwerdt, G.; Gekle, M. A rapid screening method to test apoptotic  
700 synergisms of ochratoxin A with other nephrotoxic substances. *Toxicol. In Vitro* 2005, 19, 135–143.

701 White SR, Williams P, Wojcik KR, et al. Initiation of apoptosis by actin cytoskeletal derangement in  
702 human airway epithelial cells. *American Journal of Respiratory Cell and Molecular Biology*.  
703 2001;24(3):282–294.

704 Yamazaki Y, Tsuruga M, Zhou D, Fujita Y, Shang X, et al. (2000) Cytoskeletal disruption accelerates  
705 caspase-3 activation and alters the intracellular membrane reorganization in DNA damage-induced  
706 apoptosis. *Exp Cell Res* 259: 64–78.